Received: December 19, 2022 Revised: March 16, 2023 Accepted: March 29, 2023

https://doi.org/10.1016/j.neurom.2023.03.018

On-Off and Proportional Closed-Loop Adaptive Deep Brain Stimulation Reduces Motor Symptoms in Freely Moving Hemiparkinsonian Rats

Judith Evers, PhD[1]; Jakub Orłowski, PhD[1]; Hanne Jahns, PhD[2]; Madeleine M. Lowery, PhD[1]

ABSTRACT

Objectives: Closed-loop adaptive deep brain stimulation (aDBS) continuously adjusts stimulation parameters, with the potential to improve efficacy and reduce side effects of deep brain stimulation (DBS) for Parkinson's disease (PD). Rodent models can provide an effective platform for testing aDBS algorithms and establishing efficacy before clinical investigation. In this study, we compare two aDBS algorithms, on-off and proportional modulation of DBS amplitude, with conventional DBS in hemiparkinsonian rats.

Materials and Methods: DBS of the subthalamic nucleus (STN) was delivered wirelessly in freely moving male and female hemiparkinsonian ($N = 7$) and sham ($N = 3$) Wistar rats. On-off and proportional aDBS, based on STN local field potential beta power, were compared with conventional DBS and three control stimulation algorithms. Behavior was assessed during cylinder tests (CT) and stepping tests (ST). Successful model creation was confirmed via apomorphine-induced rotation test and Tyrosine Hydroxylase–immunocytochemistry. Electrode location was histologically confirmed. Data were analyzed using linear mixed models.

Results: Contralateral paw use in parkinsonian rats was reduced to 20% and 25% in CT and ST, respectively. Conventional, on-off, and proportional aDBS significantly improved motor function, restoring contralateral paw use to approximately 45% in both tests. No improvement in motor behavior was observed with either randomly applied on-off or low-amplitude continuous stimulation. Relative STN beta power was suppressed during DBS. Relative power in the alpha and gamma bands decreased and increased, respectively. Therapeutically effective adaptive DBS used approximately 40% less energy than did conventional DBS.

Conclusions: Adaptive DBS, using both on-off and proportional control schemes, is as effective as conventional DBS in reducing motor symptoms of PD in parkinsonian rats. Both aDBS algorithms yield substantial reductions in stimulation power. These findings support using hemiparkinsonian rats as a viable model for testing aDBS based on beta power and provide a path to investigate more complex closed-loop algorithms in freely behaving animals.

Keywords: 6-OHDA rat, adaptive deep brain stimulation, closed-loop, deep brain stimulation, Parkinson's disease

INTRODUCTION

Closed-loop deep brain stimulation (DBS), commonly termed adaptive DBS (aDBS), adjusts stimulation parameters on the basis of biomarkers of pathological neural activity, promising better control of both symptoms and side effects in patients with Parkinson's disease (PD), along with extended battery life.[1–3] Local field potential (LFP) activity in the beta frequency (13–30 Hz) range has been the most commonly proposed biomarker for aDBS to date. Elevated beta activity can be detected throughout the cortico-basal

Address correspondence to: Judith Evers, PhD, Neuromuscular Systems Lab, School of Electrical and Electronic Engineering, University College Dublin Belfield, Engineering Bldg, Belfield, Dublin 4, Ireland. Email: judith.evers@ucd.ie

[1] Neuromuscular Systems Lab, School of Electrical and Electronic Engineering, University College Dublin Belfield, Belfield, Dublin, Ireland; and
[2] Department of Pathology, School of Veterinary Medicine, University College Dublin Belfield, Dublin, Ireland

For more information on author guidelines, an explanation of our peer review process, and conflict of interest informed consent policies, please see the journal's Guide for Authors.

Source(s) of financial support: This project is supported by the European Research Council (Grant Number ERC-2014-CoG-646923 646923 and 2018-POC-875516) and Horizon 2020 (Marie Sklodowska-Curie Grant 101030486).

ganglia network of individuals with PD and is a hallmark pathological feature of PD.[4] Increased local and interhemispheric synchronization accompanied by longer beta bursts has been reported during periods of clinical impairment.[5] Elevated beta activity has been shown to be reduced during DBS and is correlated with motor impairment.[5] These features, combined with the ability to record LFPs at nonstimulating contacts on the DBS lead, make LFP beta power an appealing biomarker for closed-loop DBS.

Closed-loop DBS based on subthalamic nucleus (STN) beta power has been successfully shown in humans using on-off, dual threshold, and proportional control algorithms.[6–8] Technical challenges, however, have limited the clinical application of closed-loop DBS to date. Most reported studies have examined small numbers of patients, over short periods, often within a hospital setting or during the postoperative period with the patient immobile.[6,8] Although a range of different possible control algorithms have been proposed, many based on computational studies,[9–11] a direct comparison of the performance of different control algorithms within the same population has not been reported. Long-term performance of closed-loop DBS in patients has also not yet been examined. Consequently, it is not clear whether closed-loop algorithms, particularly when extending beyond simple modulation of DBS amplitude, may cause unforeseen effects or interact adversely with other oscillations and rhythms within the brain network.

Preclinical testing in animal models offers a platform for testing the efficacy and establishing the long-term safety of different aDBS methods. It remains an important step in the pipeline for clinical translation of closed-loop DBS. Closed-loop DBS based on primary motor cortex or globus pallidus internus activity has been shown to improve akinesis in the 1-methyl-4-phenyl-1,2,3,6-tetrahydropyridine (MPTP) model in two African green monkeys,[12] and aDBS based on STN beta power, in addition to continuous DBS, has been shown to improve rigidity but not tremor in the MPTP model in one rhesus macaque.[13] Although nonhuman primates (NHP) are particularly appealing model animals because of their similarities to humans, the ethical and legal considerations of NHP studies, in addition to their increased cost, lead to low sample sizes, which is an important limitation. In contrast, the rat is particularly suitable owing to its size, availability, and the existence of an established PD model in the 6-hydroxydopamine (6-OHDA) rat model.[14] In addition, the 6-OHDA rat has been previously used to study the effectiveness of DBS,[15–17] and it exhibits enhanced beta activity, which can be used as a biomarker, although its prominence depends on alertness levels and movement state.[18–20] Finally, using wireless recording and stimulation systems allows animals to exhibit a full range of movement without being impeded by a tether.[21–23] Although the efficacy of continuous DBS has been shown in several studies,[24–28] closed-loop aDBS has not yet been evaluated in the 6-OHDA rat. To address this, the aim of this study was to examine the effect of closed-loop aDBS algorithms on motor impairment, STN beta power, and stimulation power in freely moving 6-OHDA rats. The efficacy of two closed-loop algorithms, on-off and proportional amplitude modulation, was examined and compared with that of conventional open-loop DBS.

MATERIALS AND METHODS

Rodent Study

Study Design

Adult male ($N = 8$) and female ($N = 2$) naive Wistar rats were implanted with a stimulation and recording multielectrode array (MEA) in the left STN. Rats were either rendered hemiparkinsonian by injection of 6-OHDA (PD group, $N = 7$) or sham operated (sham group, $N = 3$). One rat in each group, PD and sham, was female. A randomized block design was used. Behavioral assessment began three weeks after surgery, when the toxin model was fully developed and was performed under seven different conditions: 1) no stimulation, 2) conventional 130 Hz open-loop DBS, 3) on-off closed-loop stimulation based on STN relative beta power, 4) proportional closed-loop stimulation based on STN relative beta power, 5) randomly timed on-off stimulation (as a control for closed-loop on-off control), 6) low-amplitude stimulation at the mean, and 7) 20th percentile of the amplitude delivered during proportional control (as controls for the proportional control algorithm). Current-controlled DBS (20–100 μA) was applied to the ipsilateral STN through the implanted electrodes. For each rat, the individual stimulation amplitude was set at 80% of the stimulation-induced dyskinesia threshold.

During each recording session, the following sequence was performed. After acclimatization to the behavior room, a baseline LFP was recorded for 60 seconds, followed by selection of stimulation amplitude. Stimulation was applied for 5 minutes before commencing behavioral tests. LFP data were recorded using the MCS Experimenter software (Multi Channel Systems, Reutlingen, Germany) during each of the behavioral tests (5-minute CT, 5-minute open field test [OFT] followed by 10 minutes rest and 5-minute repeat OFT and the duration of the ST [2–3 minutes]). The behavior of the animal was simultaneously recorded using the Ethovision (Noldus, Wagenigen, The Netherlands) video tracking system. The sequence of stimulation algorithms and the order of rats were randomized.

At the end of the study (maximal 16 weeks), rats were perfused with formalin and brains harvested for histologic assessment. Analysis of histologic slides was computerized, eliminating the need for blinding. The sample size calculation with a power of 80% and α-level of 0.05 was based on[29] the estimated effect of different DBS algorithms. The primary outcome measures were the contralateral paw use in the behavioral assays, change in relative beta power in recorded LFPs, and change in the average power delivered.

Scientific animal work was approved by the University College Dublin Animal Research Ethics Committee (AREC 17-22) and licenses by the Health Product Regulatory Authority Ireland (AE18982-P122). Reporting in the animal study followed the ARRIVE 2.0 guidelines.

Animal Husbandry

Rats were housed in stable pairs for a minimum of one week before recovery surgery and stayed in those pairs after recovery surgery.[30] After surgery, rats were monitored daily for four days and three times per week thereafter. A custom score sheet including the Rat Grimace Scale,[31] a facility-specific health-score system based on clinical appearance and a score measuring motor deficits, was used for welfare assessment. Assessment and treatments followed no set order. General housing condition in a specific-pathogen–free facility included a 12/12-hour light-dark cycle in a temperature (21.6 °C ± 0.5 °C) and humidity (50.8% ± 6.1%) controlled environment and access to water and standard rodent diet ad libitum. Cages contained woodchip bedding, paper shreds, a hammock, and enrichment in the form of wooden balls or sticks and a cardboard tunnel in later blocks. Rats were fed on the ground

because the cement cap could become entangled in metal food dispensers. Cages were cleaned twice per week.

Multielectrode Array Implantation and PD Disease Model

At the time of surgery, rats weighed 377 ± 75 g and were 11.2 ± 2.2 weeks old. Stereotaxic surgery was performed under gaseous anesthesia (induction with 4.5% isoflurane in 4 l/min oxygen and maintenance with 1.2%–1.8% isoflurane in 1 l/min oxygen). The depth of anesthesia was monitored continuously using the pedal withdrawal reflex and corneal reflex. Surgical practice included temperature control using a heating blanket, an aseptically prepared surgical field, subcutaneous (s.c.) antibiosis given before and three days after surgery (Gentamicin [6 mg/kg] QD), tear replacement ointment (Vidisic, Dr Gerhard Mann, Chem.-pharm. Fabrik GmbH, Berlin, Germany), local anesthesia at the skin incision (maximum 0.05 ml 0.5% Lidocaine, diluted from Lidocaine 1%, Hameln Pharmaceuticals Ltd, Gloucester, UK), anesthetic cream at the ear bars (Emla 5% cream, AstraZeneca, Cambridge, UK) and analgesia (Buprenorphine one hour before and three days after surgery (0.015 mg/kg s.c., four times a day). With the animal placed in a stereotaxic frame (Stoelting, Dublin, Ireland) with nonrupture ear bars, a medial skin incision was made; the reference points bregma and lambda were exposed and four bone screws (1.59 mm, Stoelting) inserted. For the PD disease model, 15 µg 6-OHDA (6-Hydroxydopamine hydrobromide, Sigma-Aldrich, Arklow, Ireland), freshly prepared on the day in 0.9% saline solution with 0.01% ascorbic acid (Sigma-Aldrich) and kept in a dark vial on ice, was injected into the left medial forebrain bundle (stereotaxic coordinates: −4.0 mm craniocaudal, 1.3 mm lateromedial from bregma, and −7.0 mm dorsoventral from the dura, tooth bar at 4.5 mm) over 5 minutes, with the cannula left in place for another 10 minutes to allow diffusion. A PIIr MEA with six contacts (each contact ø 75 µm, two for stimulation, four for recording) was implanted into the left STN (stereotaxic coordinates: −3.6 mm craniocaudal, −2.5 mm lateromedial from bregma, and −7.6 mm dorsoventral from the dura). The size of the rat's skull was considered and if necessary controlled for. In the sham group, instead of the neurotoxin, the same amount of vehicle was injected and an MEA implanted. Once positioned, the MEA was fixed with cyanoacrylic glue (Loctite, Henkel, Germany), and the skull was covered with a cap of dental cement (Dentalon plus, Heraeus Kulzer GmbH, Hanau, Germany), enveloping the connector for the headstage and forming a platform to secure the headstage. The skin was realigned caudally using an intradermal suture (Vycyl 4-0, Ethicon Inc, Somerville, NJ).

Behavioral Tests

All behavioral tests were performed in a designated behavior suite before 12 PM by the same researcher. The room had a temperature of 21.4 °C ± 0.48 °C, humidity of 53% ± 4.9%, light of 12 ± 3 lux, and noise level of 42 ± dB. Behavioral tests were recorded using Ethovision XT 15 (Noldus) and a camera (Basler acAI300, Basler, Ahrensburg, Germany). The model was confirmed by apomorphine-induced rotation test. Apomorphine was injected at 0.25 mg/kg, and clockwise and counterclockwise rotations were counted in 5-minute bins for 60 minutes in an OFT box (64 × 64 cm). All animals showed at least two rotations per 5 minutes and were used (data not shown). Akinesia for each stimulation algorithm was assessed using the CT and ST. Bradykinesia was assessed using the OFT. The CT was the first test performed by each rat on each day. The rat was placed in a transparent plexiglass cylinder ø24 cm, 46 cm high) for 5 minutes. For the OFT, rats were placed in one corner of a square box (64 × 64 cm) and their movement recorded for 5 minutes. The OFT was repeated after a 10-minute rest period. For the ST, rats were moved at a speed of 90 cm in 6 seconds over the tabletop while the hind paws and one front paw were supported by the researcher. Four trials of each paw were performed while alternating the paws between trials.

Histology and Immunocytochemistry

Rats were anesthetized (induction with 5% Isoflurane in 5 l/min oxygen). Anesthesia was deep enough to abolish the pedal withdrawal reflex completely, and the animal was transcardially perfused with phosphate buffered saline (Sigma-Aldrich), followed by 10% formalin (Sigma-Aldrich), after administration of heparine (625 IU/rat, INNOHEP 2500 IU, LEO Pharma, Ballerup, Denmark). The brain was harvested for histologic assessment. The brain tissue was paraffin embedded, and 4 µm coronal slices were cut (Leica RM2135 microtome, Leica Biosystems, Newcastle, UK) for standard hematoxylin and eosin (H&E) staining and immunocytochemistry for Tyrosine Hydroxylase (TH). Immunohistochemical staining for TH was carried out on a Bond-III immunostainer (Leica Biosystems). Primary antibody TH (EMD Millipore, AB152) was diluted in Bond Primary Antibody Diluent (Leica, AR9352) at 1/100. Pretreatment of samples was carried out on the Bond-III using Bond Epitope Retrieval Solution I (Leica, AR9961) for 20 minutes. Detection and visualization of stained cells were achieved using the Bond Polymer Refine Detection Kit (Leica, DS9800) with Bond DAB Enhancer (Leica, AR9432). The tissues were counterstained with hematoxylin and cover slipped. For location of the multielectrode array, five to ten coronal slices 40 µm apart were cut in the STN area and stained with H&E. For the TH-immunocytochemistry, five coronal slices 40 µm apart were cut in either the substantia nigra or striatum area and stained for tyrosine hydroxylase. Slices were then scanned at 40× magnification (ScanScope XT, Aperio Technologies, Vista, CA) and computationally analyzed using custom-developed code in MATLAB (MathWorks, Natick, MA). The densities of stained pixels in the striatum and substantia nigra pars compacta were quantified in both hemispheres and the difference expressed as a percentage.

Data Acquisition and Stimulation System

LFP data were recorded, and DBS applied using a wireless programmable, battery-powered headstage system (W2100, Multi Channel Systems). Within the headstage, LFP data were filtered between 1 Hz and 5 kHz, amplified with a gain of 100, sampled at 20 kHz using a 16-bit analog-to-digital converter, and wirelessly transmitted to the receiver. The receiver was connected to an interface board containing a digital signal processor that was programmed to process the recorded signal and determine the stimulation to be applied using the selected feedback control algorithm. The stimulation amplitude was then updated at the headstage to apply one of up to 16 stored stimulation patterns based on the parameters determined by the control algorithm. The total delay of the closed-loop system, including wireless transmission, biomarker computation, and DBS pulse definition, was determined to be <20 milliseconds. An overview of the experimental setup is presented in Figure 1.

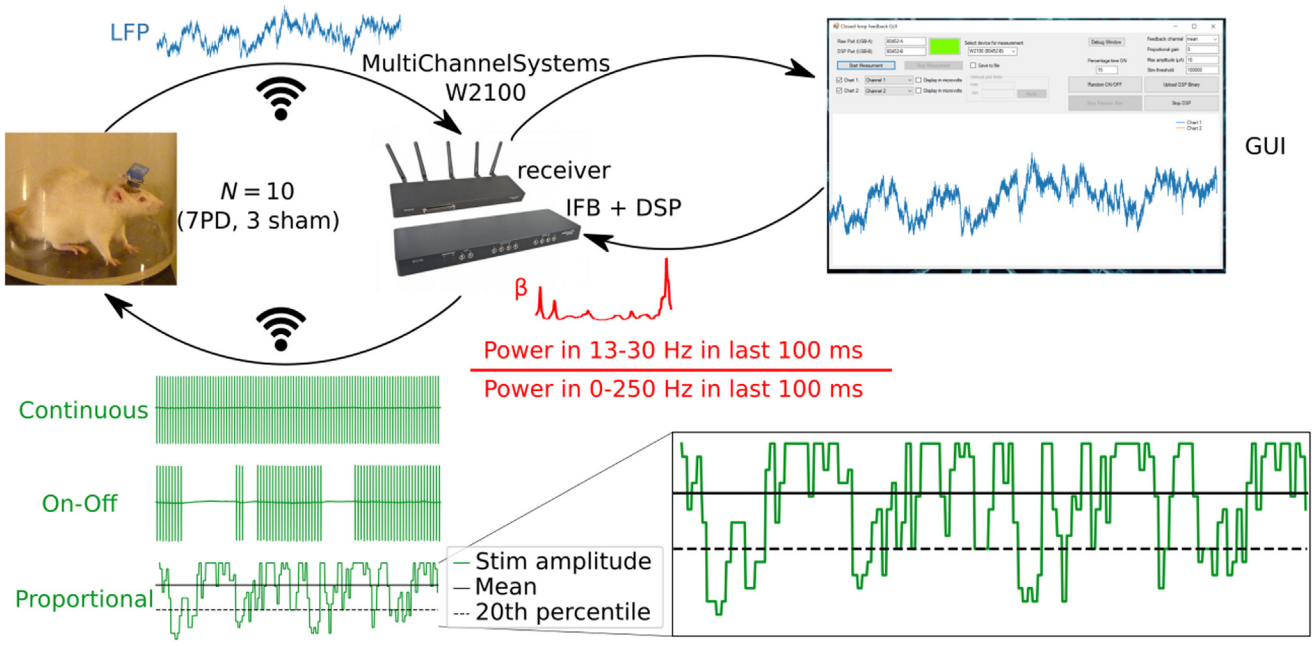

Figure 1. Schematic illustration of the closed-loop recording and stimulation setup. The signals recorded from the animals are presented in blue; the signals processed by the digital signal processor (DSP) unit present on the interface board (IFB) are presented in red; the stimulation signals are shown in green. Sample stimulation waveforms are shown for continuous, on-off, and proportionally controlled aDBS based on relative beta power. The mean and 20th percentile of the stimulation amplitude used during proportional aDBS were estimated for low-amplitude stimulation (inset). GUI, graphical user interface. [Color figure can be viewed at www.neuromodulationjournal.org]

Deep Brain Stimulation

Biomarker

DBS amplitude was modulated on the basis of the relative amplitude of the power in the beta band of the STN LFP. The relative beta power rather than absolute power was chosen as the biomarker to control for possible changes in the overall power of the signal. To obtain the biomarker, the LFP signal was first downsampled to 500 Hz using a two-step antialiasing low-pass filter (Butterworth, third order) and downsampling with zero order hold. Beta activity was extracted using a 13-to-30–Hz bandpass filter (Butterworth, sixth order). The relative beta power was estimated from the last 50 samples (100 milliseconds) as

$$\beta[n] = \frac{\sum_{i=0}^{49} x_{13;30}^2[n-i]}{\sum_{i=0}^{49} x_T^2[n-i]} \quad (1)$$

where $x_{13;30}$ is the signal bandpass filtered in the 13-to-30–Hz frequency band, and x_T is the signal before bandpass filtering.

Stimulation Paradigms

Monopolar cathodic stimulation was applied using biphasic charge balanced rectangular pulses, of equal amplitude and 80 μs duration, with a stimulation frequency of 130 Hz.[32] The following six stimulation paradigms were implemented.

Open-loop continuous stimulation, similar to that used clinically, was included as a benchmark. To set the stimulation amplitude, a stepwise approach was used for each rat, starting at 20 μA. The stimulation amplitude was set at 80% of the stimulation-induced dyskinesia threshold for each rat.

On-off stimulation was delivered intermittently, on the basis of the current value of the beta biomarker. The threshold for stimulation was set at approximately 50% of the maximum value of the biomarker measured with stimulation off. When the biomarker increased above threshold, stimulation was turned on using the same stimulation amplitude as in open-loop continuous stimulation. Stimulation remained on until the biomarker decreased below the threshold value, shown in Figure 2a.

Proportional stimulation modulated DBS amplitude proportionally to the magnitude of the beta biomarker. At each controller call, the desired stimulation amplitude, $u[t]$, was calculated as

$$u[t] = \text{sat}\left(k_p \frac{\beta[t]-\tau}{\tau}\right) \quad (2)$$

where sat is the saturation function, which limits the output between 0 and the selected maximum stimulation amplitude; u_{max}, k_p is the proportional gain; $\beta[t]$ is the current value of the biomarker, in accordance with Equation (1), and τ is the stimulation threshold. This allowed the stimulation amplitude to change in the predefined range proportionally with the difference between the stimulation threshold and the current biomarker value. The threshold τ in the experiments was set to 0.1%, to obtain a high level of beta suppression. To enable fast application of the selected stimulation amplitude, 16 different stimulation patterns were stored locally within the headstage. The actual stimulation amplitude was selected by rounding $u[t]$ to the nearest of the 16 predefined values. Stimulation amplitude was therefore adjusted in

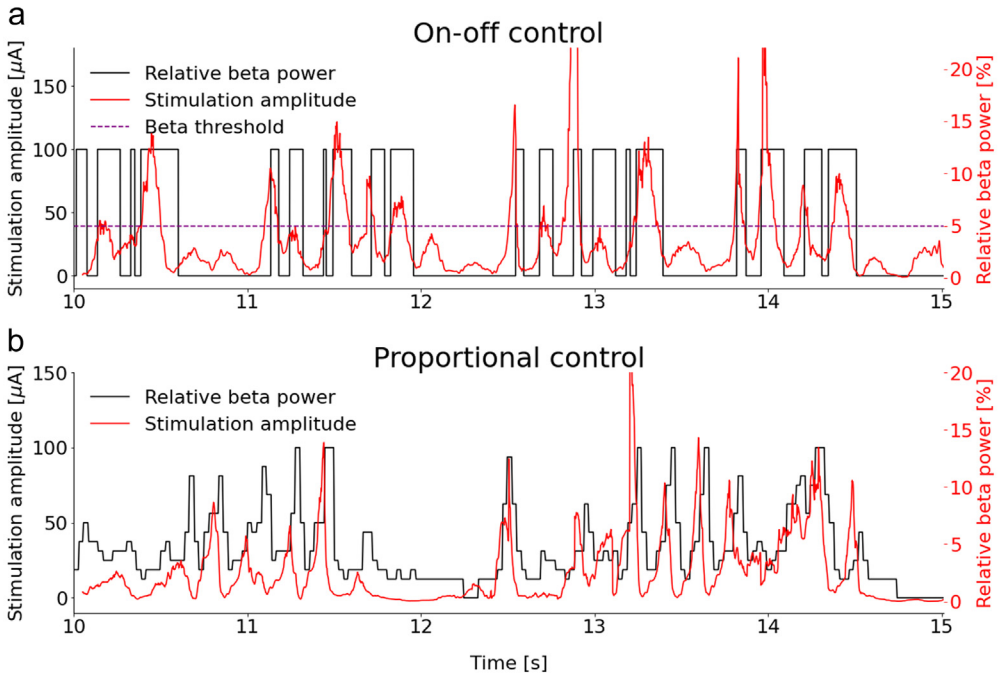

Figure 2. Illustration of proportional and on-off control modulating the DBS stimulation amplitude based on the biomarker values in a representative animal. The maximum stimulation amplitude for this rat was set to 100 μA. The relative beta power was computed offline on the basis of the recorded LFP using the same filtering and downsampling techniques as in the online system and then smoothed with a 100-millisecond moving average window. The displayed values are shifted by 50 milliseconds to the midpoint of the moving average window. a. For the on-off algorithm, the stimulation has a predefined amplitude of 100 μA (black line) when the beta power (red line) is above threshold (purple dashed line). b. For the proportional algorithm, the stimulation amplitude (black) is updated proportionally to the relative beta power (red line). The maximum value of the stimulation amplitude during this recording session was set to 100 μA. [Color figure can be viewed at www.neuromodulationjournal.org]

linearly spaced discrete steps from 12.5% to 100% of the maximum stimulation amplitude u_{max} (Fig. 2b) and turned off completely when the biomarker value fell below threshold.

The stimulation amplitude was updated approximately every 30 milliseconds during on-off and proportional stimulation and kept constant between the updates.

To verify that the effects of the stimulation were due to the closed-loop nature of the system, three more control algorithms were implemented.

Random on-off stimulation delivered a stimulation pattern equivalent to that applied during on-off stimulation, though with stimulation applied at randomly chosen times. Stimulation was sequentially turned on and off, with the duration of each interval of stimulation selected randomly, with uniform distribution, between 1 and 220 milliseconds, and the duration of each interval "off" stimulation selected between 1 and 513 milliseconds. This resulted in stimulation being on for approximately 43% of the recording, to match the average distribution from the first on-off recordings.

Low-amplitude continuous stimulation. To verify that the effects of the proportional stimulation were due to the controller responding to changes in the biomarker rather than stimulation at a minimum threshold, above which the amplitude was modulated, continuous stimulation was applied at one of the two reduced amplitudes compared with the amplitude used in the open-loop stimulation experiments. The values were selected to match the mean and the 20th percentile of the stimulation amplitude used during proportional stimulation performed on the same rat.

Data Analysis

Behavioral Data

For the CT, each touch of a paw (left, right, or both) on the vertical walls was noted. Only trials with a minimum of ten wall touches were used in the analysis. The ratio between ipsi- and contralateral paw use was reported. For the ST, the number of adjustment steps the rat made was counted for each paw. The average of all four trials was presented as a ratio of ipsi- and contralateral forepaw use. Counting for the CT and ST was performed by one researcher (Judith Evers) blinded to the stimulation protocol, with the video playing at half speed. The distance travelled in the OFT was extracted from Ethovision (Noldus).

Analysis of Local Field Potentials

Of 602 LFP recordings, 53 were discarded owing to the presence of excessive stimulation artifacts or noise. Ten signals were discarded owing to 50-Hz power line noise that masked the underlying LFP, 28 owing to strong stimulation artifacts in the beta band, ten owing to an absence of visible LFP activity in the recording, and five owing to recording quality issues (baseline drift, breaks in the recording, saturation). For each of the remaining 549 recordings, the power spectrum of the signal was estimated using Welch's method (Hanning window, 2-second length, 50% overlap), and a straight line was fitted to the log-log transform of the resulting spectrum in the 2-to-100–Hz range to obtain an estimate of the $1/f^n$ component. The detrended power spectra in the 13-to-30–Hz range after subtraction of the $1/f^n$ background component were then examined. In all the baseline recordings ($N = 138$), the most

prominent peak was visually identified in a double-blind setting by two researchers (Judith Evers and Jakub Orłowski) independently. When the researchers did not agree ($N = 21$), the peak was selected on the basis of its prominence relative to average activity in the adjoining frequency bands. The power within a 4-Hz band centered on the beta peak (14–18 Hz, Effect of Stimulation on Spectral Power section), P_β, and the total power, P_T, in the 10-to-100–Hz frequency range were then estimated. Power at frequencies <10 Hz was ignored to minimize the influence of $1/f^n$ background noise (STN LFP Beta Oscillations in 6-OHDA Rats section). A similar procedure was applied to obtain relative power in the alpha (7–10 Hz), high beta (20–40 Hz), and gamma (60–90 Hz) bands, with the power in the alpha band normalized regarding the power in the 2-to-100–Hz range. The relative beta power in each recording was estimated as the ratio of P_β/P_T and compared with the same quantity from the baseline recording obtained for the same day and the same rat (Fig. 3).

Stimulation Power

The power delivered during continuous stimulation was estimated as

$$P_{\text{stim}} = I^2 \cdot pw \cdot f \cdot Z \quad (3)$$

where I is the stimulation current, pw is the pulse width, f is the stimulation frequency, and Z is the electrode impedance.[33] For on-off and proportional stimulation, with time-varying amplitude, the power was estimated for each period of constant amplitude, scaled by the length of that period, summed, and normalized by the length of the recording to obtain the average power.

Statistical Analysis

The baseline (no stimulation) in 6-OHDA and sham groups was first compared using a one-tailed t-test to confirm presence of behavioral symptoms of PD in the model. Linear mixed model analysis was used to assess the influence of stimulation algorithm on contralateral paw use in CT and ST, distance travelled in OFT, the $1/f^n$ activity and relative alpha, beta (low and high), and gamma power. Separate models were fitted to assess each feature and group. The fixed effect for each model was stimulation, with animals included as a random intercept term.[34] Main effects were compared using Satterthwaite's method,[35] and post hoc tests were conducted using estimated marginal means applying a Tukey correction for multiple comparisons[36] (R, version 1.7.2). The location of the beta frequency peak in the LFP power spectrum also was compared across stimulation conditions, using a linear mixed model with the fixed-effect group and subject as a random intercept term. Statistical analysis was conducted in R version 4.1.215 using the lmer (Bates), lmerTest (Kuznetsova), and emmeans (Lenth) libraries.

RESULTS

Behavioral Tests

Rats in the 6-OHDA group had reduced use of their paw contralateral to the injection side in the CT (t[33] = 8.17, $p < 0.0001$) and ST (t[34] = 6.65, $p < 0.0001$) and travelled less in the OFT (t[70] = 2.37, $p = 0.01$), confirming the presence of parkinsonian motor impairments. In both CT and STs, continuous, on-off, and proportional DBS significantly improved contralateral paw use (Fig. 4a,c). In contrast, neither random on-off DBS nor continuous DBS at the mean amplitude or 20th percentile of proportional aDBS was effective (Fig. 4a,c). Linear mixed model analysis confirmed a significant effect of stimulation algorithm (F[94.34] = 24.7, $p < 0.001$ and F[97.20] = 34.9, $p < 0.001$ for CT and ST, respectively, post hoc tests in Supplementary Data Tables S1 and S2). In the sham group, contralateral paw use was approximately 50%, and no significant effect of stimulation was observed (Fig. 4b,d, F[21] = 0.001, $p = 0.999$ and F[21] = 0.56, $p = 0.64$ for CT and ST, respectively, Supplementary Data Tables S1 and S2). Stimulation had no effect on the distance traveled for any stimulation algorithm in the 6-OHDA group (linear mixed model: F[197.4] = 1.21, $p = 0.30$, data not shown).

STN LFP Beta Oscillations in 6-OHDA Rats

The average power spectrum of all the baseline recordings from the 6-OHDA rats is presented in Figure 5a, and example power spectra from one 6-OHDA and one sham rat are presented in Supplementary Data Figure S5. A clear peak is visible at approximately 15 Hz in the average power spectrum of the 6-OHDA rats, though not in the average spectrum of the baseline recordings from the sham rats (Fig. 5b). The average spectra estimated individually for each rat are presented in Supplementary Data Figure S2. A linear mixed model was used to analyze differences in relative beta power between the 6-OHDA and sham group. There was no significant difference between the two groups (F[9.49] = 1.13, $p = 0.31$). The frequency at which the maximum peak within the beta frequency band occurred in the LFP power spectrum of the baseline recordings is presented in Figure 5c. In the 6-OHDA rats, a peak within the beta frequency range was consistently observed in the power spectrum of the STN LFP. In 85% of recordings, the peak occurred in the low beta frequency (14–18 Hz) range. In contrast, the sham rats did not preferentially exhibit a peak within the low beta range (52% of the peaks fell in this range), and the location of the most prominent peak was approximately uniformly distributed throughout the beta range. The distribution of the peak locations was significantly different between the 6-OHDA and control rats (Fig. 5c). The kurtoses of the two distributions (1.11 for 6-OHDA rats and 0.18 for sham rats) differ significantly, as confirmed by a two-sample Kolmogorov-Smirnov test (D[14, 20] = 0.75, $p < 0.001$).

$1/f^n$ Noise increased during stimulation, regardless of the algorithm used (Supplementary Data Figure S1). The increase in $1/f^n$ noise during beta-triggered on-off stimulation and random on-off stimulation was less than that during continuous stimulation or proportional stimulation (linear mixed model: F[6533.87] = 168.45, $p < 0.001$, post hoc tests in Supplementary Data Table S3).

Effect of Stimulation on Spectral Power

In the 6-OHDA rats, the relative power in the STN LFP beta band decreased with stimulation compared with the rat-and-day–matched baseline recording, regardless of the algorithm used (linear mixed model: t[363.09] = 108.7, $p < 0.001$ and post hoc tests in Supplementary Data Table S4, Fig. 3a). No reduction was observed in the sham rats (linear mixed model: t[39.1] = 0.43, $p = 0.09$, Fig. 3b).

The amount of suppression of beta activity, however, depended on the stimulation algorithm. Lower levels of suppression of beta

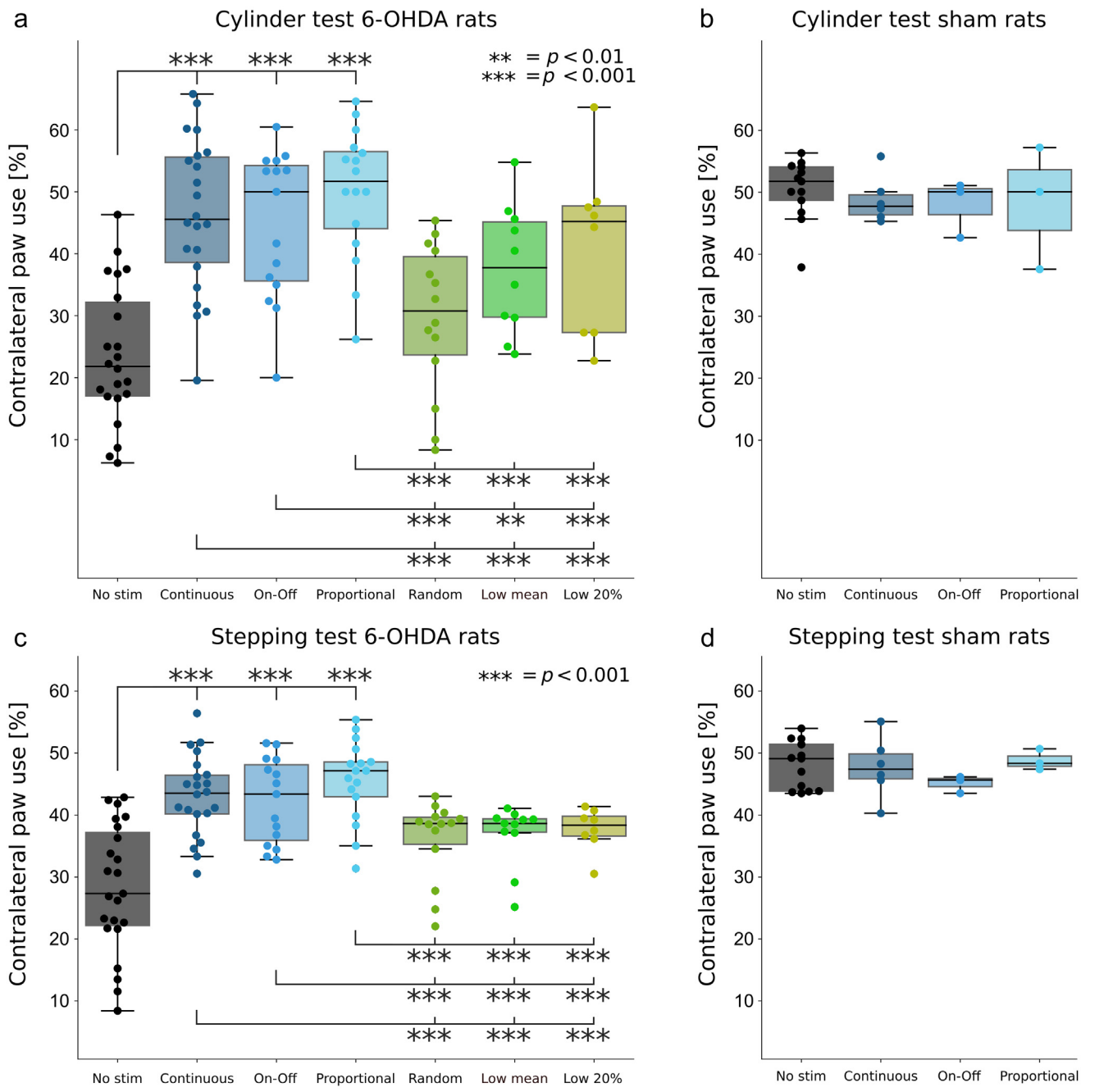

Figure 3. Change of relative beta as regards the baseline for 6-OHDA and sham rats under various stimulation algorithms. a. Beta power compared with rat-and-day–matched baseline beta in 6-OHDA rats. DBS, regardless of modality, suppresses the relative beta power in hemiparkinsonian rats. b. DBS does not change the relative beta level in sham rats compared with baseline, regardless of the stimulation algorithm. [Color figure can be viewed at www.neuromodulationjournal.org]

activity were observed for the on-off and random algorithms than for continuous stimulation (continuous, mean low, and 20% low) and proportional stimulation. The level of beta suppression was significantly different during continuous and proportional control when compared with the intermittent stimulation protocols, $p < 0.01$ for all pairwise comparisons (Supplementary Data Table S4).

Relative power in the high beta band was reduced during stimulation compared with no stimulation for all stimulation paradigms in the 6-OHDA group (linear mixed model: t[431.82] = 19.58, $p < 0.001$ and post hoc tests in Supplementary Data Table S5, Supplementary Data Fig. S6a). In the sham group only, on-off aDBS and continuous DBS reduced relative power in the high beta band (linear mixed model: t[49.35] = 4.94, $p = 0.004$ and post hoc tests in Supplementary Data Table S5, Supplementary Data Fig. S6b).

Relative power in the alpha band (7–10 Hz) decreased under stimulation compared with no stimulation in the 6-OHDA but not in the sham group (6-OHDA group linear mixed model: t[432.03] = 139.66, $p < 0.001$ and post hoc tests in Supplementary Data Table S6, Supplementary Data Fig. S7a, and sham group linear

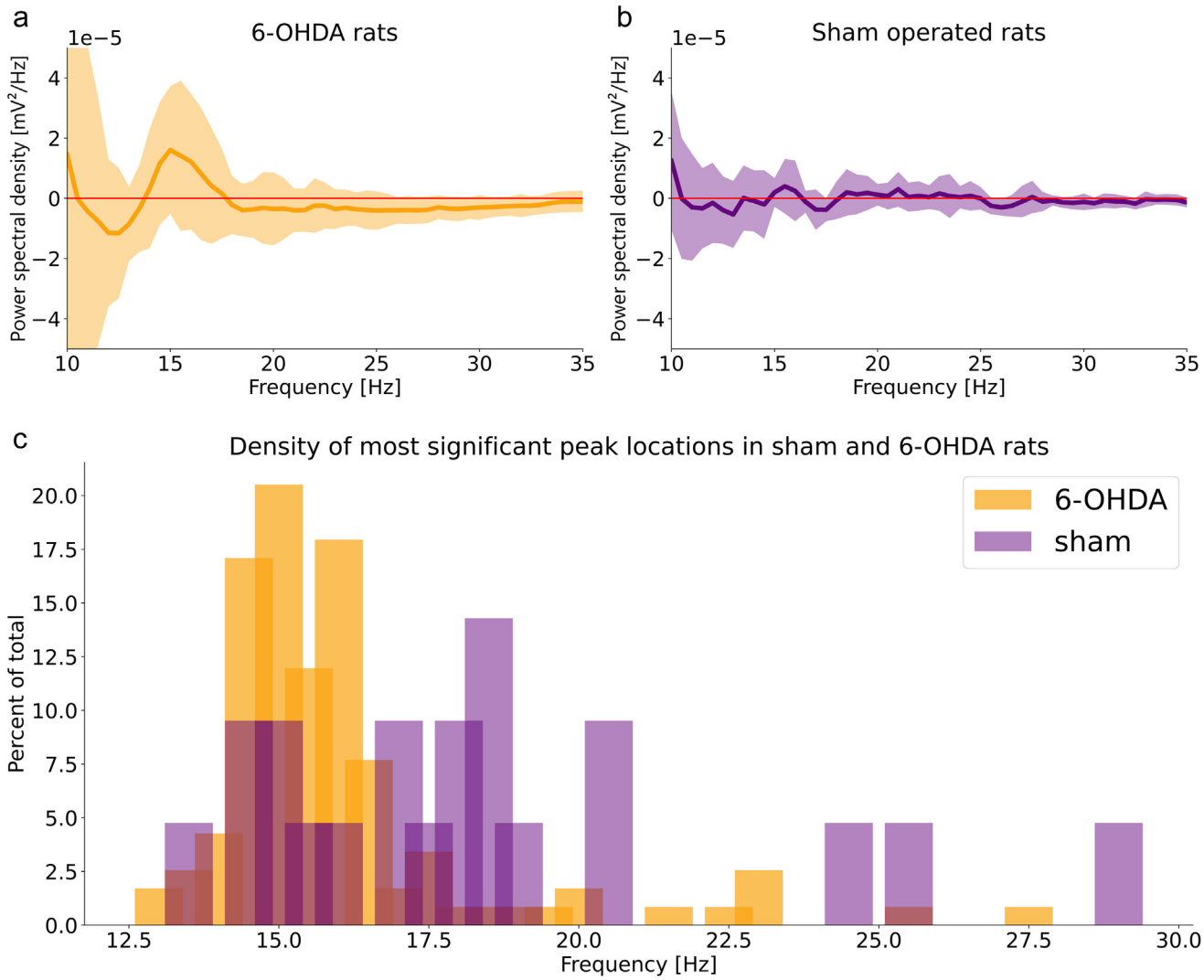

Figure 4. Behavioral results from 6-OHDA and sham rats during the cylinder test and stepping test. Continuous, β-driven on-off and proportional aDBS resulted in significant improvements in contralateral paw use in 6-OHDA rats, whereas random on-off stimulation and low-amplitude continuous stimulation did not. In the sham rats, contralateral paw use remained at approximately 50%, regardless of the stimulation algorithm. [Color figure can be viewed at www.neuromodulationjournal.org]

mixed model: t[39.57] = 35.62, p = 0.225, and post hoc tests in Supplementary Data Table S6, Supplementary Fig. S7b).

In the gamma band (60–90 Hz), relative power was increased during all stimulation paradigms compared with no stimulation. There also were two groups in which a more substantial increase was observed in gamma in the continuous stimulation paradigms (continuous, proportional, and low amplitude) than in the intermittent paradigms (on-off and random) (linear mixed model: t[430.51] = 164.79, $p < 0.001$ and post hoc tests in Supplementary Data Table S7, Supplementary Data Fig. S8a). In the sham group, the linear mixed model revealed significant differences. In post hoc tests, these were limited to the comparison between continuous stimulation and no stimulation (linear mixed model: t[55.14] = 6.61, p = 0.0002, and post hoc tests in Supplementary Data Table S7, Supplementary Data Fig. S8b).

Power Delivered During aDBS

The average power delivered for each stimulation protocol was estimated as described in the Analysis of Local Field Potentials section 2.4.2. The results were compared with the power delivered during continuous stimulation at the same amplitude for on-off stimulation, or with maximal stimulation amplitude for proportional stimulation (Fig. 6). Both on-off and proportional algorithms resulted in substantial power savings compared with continuous stimulation, while alleviating symptoms (Behavioral Tests section). The average power delivered during on-off stimulation was 39.38% ± 21.84% of that delivered during continuous stimulation at the same amplitude. The average power delivered during proportional control was 43.61% ± 26.45% of that delivered during continuous stimulation at the maximum amplitude of the proportional stimulation.

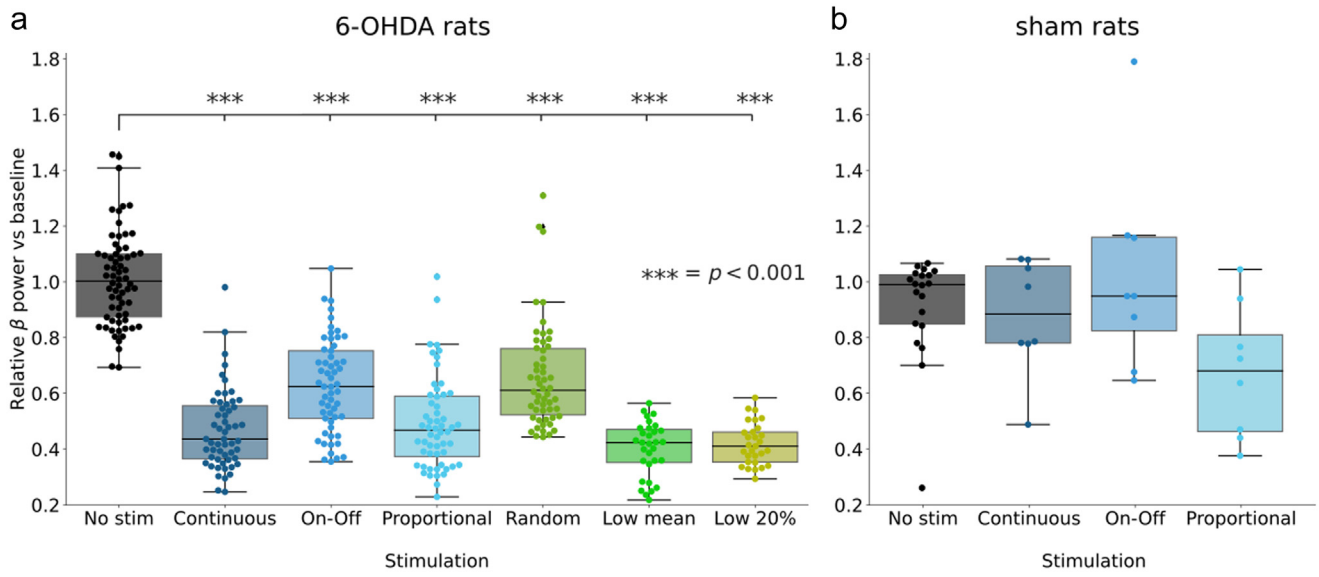

Figure 5. Location of the maximum peak in the beta (13–30 Hz) range of the detrended (not normalized) STN LFP power spectra in 6-OHDA and sham rats under baseline (no stimulation) conditions. a. Averaged detrended power spectrum from all baseline recordings from 6-OHDA rats with a prominent peak at 15 Hz. The thick line in the middle indicates the mean; the shaded region corresponds to ± 1 SD. b. Averaged detrended power spectrum from all baseline recordings from sham-operated rats, showing no consistent peak in the beta range. c. Density of locations of the most significant peak in the baseline recordings from both 6-OHDA and sham rats. The height of the bars corresponds to percentage of the peaks with a given value present in the whole data set. The value of most significant peak for 6-OHDA rats falls preferentially in the low beta (14–18 Hz) range, whereas no such grouping is present in the data from sham rats. [Color figure can be viewed at www.neuromodulationjournal.org]

Confirmation of Multielectrode Array Position and Loss of Dopaminergic Neurons

Histology confirmed that the multielectrode array was located within the STN in all ten rats (Fig. 7b, example in Supplementary Data Fig. S4). TH levels were significantly reduced by 55% ± 19% in the substantia nigra pars compacta and 67% ± 33% in the striatum in the left hemisphere in 6-OHDA treated rats, and were similar between both hemispheres in the sham group (−7% ± 11% and −9% ± 8%, respectively; one-tailed *t*-test: t[8] = 3.97, $p = 0.002$ and t[8] = 2.88, $p = 0.01$, respectively), shown in Figure 7a, examples in Supplementary Data Figure S3.

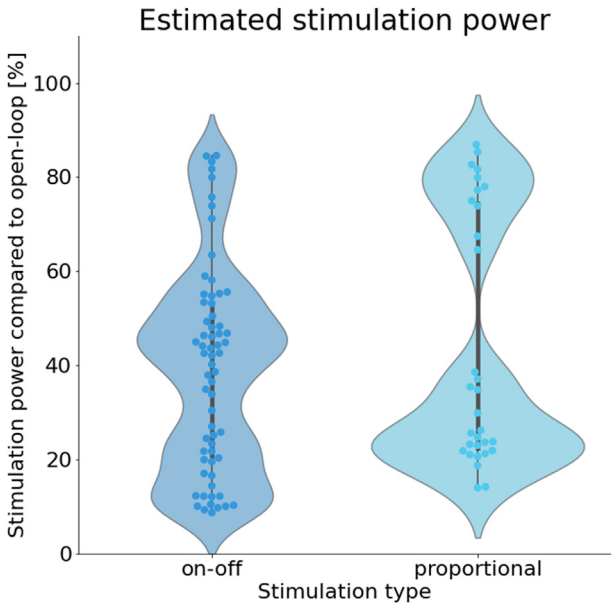

Figure 6. Normalized power delivered during on-off and proportional stimulation. The power is normalized relative to the power delivered during continuous stimulation. The 100% value indicates the power delivered during continuous stimulation of the same amplitude (on-off stimulation) or equal to the maximum stimulation amplitude (for proportional stimulation). [Color figure can be viewed at www.neuromodulationjournal.org]

DISCUSSION

In this study, closed-loop aDBS was implemented in freely moving parkinsonian rats using a wireless recording and stimulation system. Motor behavior was compared during conventional open-loop DBS and aDBS targeted at suppressing STN LFP beta band power. Closed-loop DBS using either on-off or proportional amplitude modulation was found to be as effective in suppressing PD-like motor symptoms in rats as conventional DBS (Fig. 4) with substantially reduced power.

STN LFP Beta Activity

A consistent low-amplitude peak in the low beta frequency range (14–18 Hz) of the STN LFP power spectrum was observed in all 6-OHDA rats (Fig. 5, Supplementary Data Fig. S2). Although the prominence and location of the peak were affected by day-to-day variability, the beta activity remained effective as a biomarker for aDBS. Beta band power was successfully suppressed by DBS (Fig. 3); however, only those closed-loop aDBS algorithms driven by the beta activity resulted in an improvement in motor behavior (Fig. 4).

Prominent and consistent peaks in the high and low beta frequency band have been reported in the basal ganglia in 6-OHDA rats across a range of experimental conditions.[18,19,37] Avila et al[18] and Brazhnik et al[19] reported a peak in the high beta range

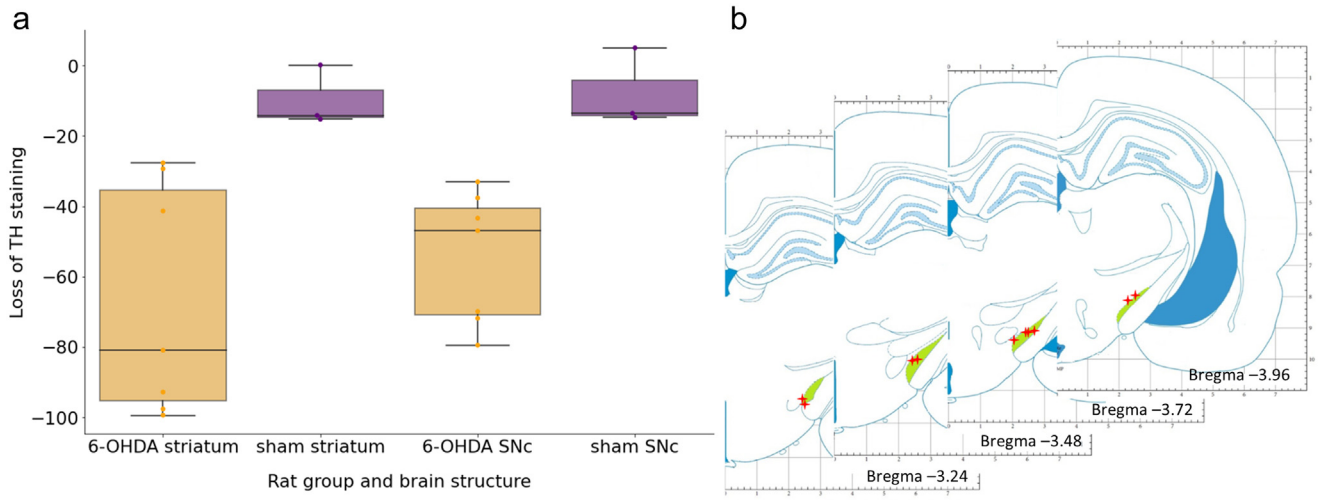

Figure 7. a. Percentage loss of TH in left substantia nigra pars (SNc) compacta and striatum in 6-OHDA and sham rats. b. Location of multielectrode array within the STN. [Color figure can be viewed at www.neuromodulationjournal.org]

(30–35 Hz) in the substantia nigra pars compacta during a walking task but absent during REM sleep and under urethane anesthesia in the presence of a sensory stimulus. Mallet et al[37] showed a peak in the lower beta range (20 Hz) in the STN of anaesthetized rats. The 6-OHDA model in their study was more severely expressed than in this study, with at least 25 rotations per minute in the rotation test. In other studies in which the model expression was milder, similarly to the present study, less prominent peaks have also been observed.[38,39] The STN LFP in 6-OHDA rats in one study[40] shows higher variability in beta activity, with less prominent peaks. Sharott et al[41] reported a low-amplitude peak in the 25-to-30–Hz range in 80% of 6-OHDA rats at rest, whereas Mottaghi et al[42] reported a low-amplitude peak in the low beta range (13–21 Hz) during rearing and both low and high beta (21–30 Hz) frequency peaks during movement in the open field chamber or treadmill but not during stepping. Our results, showing a low-amplitude peak in the low beta (14–18 Hz) range while the rat was freely moving, are thus consistent with previously established observations.

Comparison across studies is further complicated by observations that the amplitude and frequency of pathological oscillations vary with behavioral task performed by the rat.[18,19,42,43] Avila et al[18] observed an increase in high beta activity during movement, whereas low beta was decreased during the walking task. In a study by Mottaghi et al,[42] similarly, only high beta, not low beta, further increased with increasing movement speed on the rotarod. In patient studies, suppression of STN beta power before movement onset is consistently observed, including during hand movements,[44] finger tapping,[45] walking, and cycling[46] and in go/no-go tasks.[47] In our study, behavioral tests comprising both movement and rest phases have been combined and assessed together.

The well-established suppression of beta power with movement has led to concerns that beta activity may not be a suitable control variable for aDBS during movement. However, this study indicates that the relative power in the beta band is a suitably robust biomarker even during movement tasks in the rodent model.

Further analysis of the relative power across different spectral bands revealed a simultaneous reduction in relative alpha, low, and high beta power, and an increase in relative gamma power with DBS (Supplementary Data Figs. S6–8). Similar changes have been observed in patients with PD in the contralateral STN.[48] Suppression of power in the alpha and beta band has also been reported in a different study in patients and hemiparkinsonian rats under effective stimulation paradigms.[49]

Behavioral Improvement

Both closed-loop aDBS and conventional DBS improved parkinsonian motor symptoms in the 6-OHDA rats to a comparable degree. In contrast, none of the three control stimulation protocols resulted in improvements in the behavioral tests. To our knowledge, this is the first report of wireless closed-loop STN DBS in rats. McNamara et al[50] recently successfully implemented a phase-based control algorithm in tethered rats in which amplification and suppression of beta activity were achieved by stimulating in the descending or ascending phase of beta, respectively. This also translated into animal movement speed that decreaased during beta-amplifying stimulation.

The efficacy of open-loop STN DBS in reversing Parkinson-like motor symptoms in the rat has been reported for a range of behavioral outcomes.[24–28] In our study, contralateral paw use in parkinsonian rats decreased to 20% in CT and 25% in STs. This reduction was ameliorated by conventional, closed-loop on-off and proportional aDBS, restoring contralateral paw use to approximately 45% (Fig. 4). Neither randomly timed on-off nor low-amplitude continuous stimulation was as successful at restoring stepping behavior (Fig. 4). In line with our own findings, unilateral DBS has been shown to improve contralateral front paw use in the CT to healthy or near-healthy levels.[25–27] Bilateral open-loop DBS has a similar effect, restoring front limb mobility in the CT in bilaterally lesioned animals.[24] During the ST, Yu et al[28] reported a normalization of mildly impaired contralateral forepaw use with 130-Hz but not 20-Hz DBS.

The distance traveled in the OFT was lower in 6-OHDA rats than in sham rats, but no significant change in the OFT was observed for any of the stimulation algorithms examined. In previous studies, an alleviation of bradykinesia has been reported in some cases,[24,51] whereas others have not observed increased mobility during DBS[16,52] or have observed a reduction in distance traveled for certain stimulation conditions only[16] (bipolar electrodes only at

three days and three weeks). Performance in the OFT has a high variability, is subject to habituation, and is affected by many environmental parameters[53] and therefore may not be a suitable outcome measure for behavioral improvement under DBS.

Nonmotor symptoms and stimulation-induced side effects were not assessed in this study, but no dyskinesias or severe side effects, such as epileptic seizures, were noted during stimulation.

Suppression of Relative Beta Power During aDBS

Relative power in the STN LFP beta band was suppressed for all stimulation protocols considered (Fig. 3). The level of suppression was lower during intermittent stimulation protocols (on-off, random on-off) than during continuous and proportional stimulation, even when the amplitude of continuous stimulation was insufficient to yield improvements in motor function. The degree of behavioral improvement under stimulation was decoupled from the level of beta suppression. Polar et al[26] similarly showed a reduction in pathological cortical beta power with STN DBS in 6-OHDA rats, independent of the therapeutic efficacy of DBS parameters used. These results suggest that suppression of beta power alone may not be sufficient to restore function, but that behavioral improvements may be related to alterations in the dynamic behavior of pathological beta activity and that the timing of the applied stimulation plays an important role in determining therapeutic efficacy. It is possible that motor impairment is correlated with longer duration beta bursts, as reported in humans by Tinkhauser et al,[5] and that these pathological beta bursts were targeted in closed-loop on-off and proportional aDBS. The time window over which the biomarker was estimated (100 milliseconds) causes the system to respond preferentially to longer beta bursts, leaving shorter physiological bursts intact.

The observation that intermittent stimulation yielded lower levels of beta suppression than did continuous or proportional stimulation is mirrored in the $1/f^n$ component of the power spectrum (Supplementary Data Fig. S1), in which an overall increase in the background activity was observed during stimulation, regardless of the algorithm. The origin of $1/f^n$ activity within the LFP is not clear, with a range of possible sources suggested, including electrical properties of brain tissue,[54] low-pass filtering of the dendrites,[55] or noise within the data acquisition system.[56] Regardless of the source, it is possible that the increase in broadband power could mask the beta suppressing effect of DBS or alter the level of suppression of relative beta power observed. Although $1/f^n$ activity was removed during postprocessing to compare the suppression of relative beta power across stimulation protocols, it was not removed from the biomarker used for closed-loop control in real time. Changes in background activity within the beta band may thus have contributed to the biomarker during real-time implementation of the closed-loop control protocols. Although this could potentially alter the relationship between pathological beta activity and stimulation, effective control of motor symptoms was only observed during conventional open-loop DBS and during on-off and proportional stimulation that were driven by the change in biomarker, confirming the effectiveness of the closed-loop protocols.

The aDBS algorithms explored in this study were limited to on-off and proportional modulation with the target to achieve almost complete suppression of beta activity. Complete suppression of beta activity might not be needed for symptom improvement, and thus, suppression to a specific target might further refine aDBS and further reduce stimulation intensity in addition to power consumption. This is supported by studies in humans using an on-off and dual threshold approach that provided therapeutic efficiency while maintaining beta power below a fixed limit or within a predefined range.[7]

Power Delivered

Significant improvement in motor symptoms was achieved with aDBS while delivering 39.38% ± 21.84% of the power used during conventional open-loop DBS with on-off stimulation and 43.61% ± 26.45% with proportional stimulation (Fig. 6). This agrees with human studies using on-off DBS, in which overall reduction in stimulation time by approximately 55% was reported.[8,57] During proportional stimulation, a bimodal distribution of the estimated power, normalized as regards the power delivered during continuous stimulation, was observed. The bimodal distribution reflects two different groups, one in which the maximum stimulation amplitude, corresponding to 80% of the motor threshold, ranged from 90 to 100 μA and one in which it ranged from 30 to 45 μA. In the latter group, with a relatively narrow therapeutic window, the reduction in power relative to continuous stimulation was thus considerably lower. When the power consumption is compared for each rat, a significant reduction in estimated power delivered is observed; the values presented in Figure 6 are thus conservative estimates of the potential power saving of aDBS. The power delivered has been estimated on the basis of the stimulation waveform parameters and electrode impedance. It should be noted that these do not correspond to the power consumption of the closed-loop stimulation device because this will depend on additional factors such as the power required by the sensing and stimulation device to estimate the biomarker and adjust the stimulation parameters in real time.[58] However, the large reduction in power delivered offers considerable possibilities for extending the battery life of the implantable devices and adding more features such as higher signal processing capability or external connectivity.

6-OHDA Model of aDBS

The results support the use of aDBS in freely behaving 6-OHDA rats as a suitable model for preclinical testing of closed-loop DBS algorithms. Although both the on-off[8] and proportional[6,59] amplitude modulation protocols have been experimentally trialed in patients, these represent relatively simple closed-loop algorithms. Alternative algorithms offer the potential for more advanced function including adaptive control and simultaneous control of multiple biomarkers. Proportional, integral, and derivative control,[9] model-based control,[10] and dual-loop adaptive approaches[11,60] show promising results in restoring the brain activity to a non-parkinsonian state in computational models. As the complexity of the stimulation protocols increases, there is a need for suitable models for preclinical testing before trialing in patients.

The model presented here offers the advantage of enabling direct comparison of different aDBS algorithms in addition to quantification of their efficacy under a range of behavioral conditions. In this way, the relative strengths and shortcomings of various aDBS approaches can be explored and examined before testing in patients.

The wireless platform used here can be easily adapted for testing more advanced control schemes and would further benefit from miniaturization of the device and extended capacity of the battery to allow long-term recording in freely moving animals.

CONCLUSIONS

In this study, we have shown that on-off and proportional aDBS based on STN beta activity restores motor function in hemiparkinsonian rats during standard behavioral tests. Protocols that delivered equivalent levels of intermittent stimulation at time points unrelated to current beta activity or that delivered continuous stimulation at the mean proportional control amplitude were not effective in restoring function. Suppression of beta activity was observed during all stimulation protocols, including those that did not yield improvements in function. The results support using aDBS in freely behaving 6-OHDA rats as a suitable model for preclinical testing of closed-loop DBS algorithms.

Acknowledgements

The authors thank Karthik Sridhar, Adil Dahlan, and Jeremy Liegey for their technical support, and Jens Pätzold from Multi Channel Systems for help with the W2100 hardware.

Data Availability

Data are available from the corresponding author on reasonable request.

Authorship Statements

Judith Evers, Jakub Orłowski, and Madeleine M. Lowery designed the study. Judith Evers and Jakub Orłowski conducted the study, including data collection and data analysis. Judith Evers and Jakub Orłowski prepared the manuscript draft with important intellectual input from Madeleine M. Lowery. All authors approved the final manuscript.

Conflict of Interest

The authors reported no conflict of interest.

How to Cite This Article

Evers J., Orłowski J., Jahns H., Lowery M.M. 2024. On-Off and Proportional Closed-Loop Adaptive Deep Brain Stimulation Reduces Motor Symptoms in Freely Moving Hemiparkinsonian Rats.
Neuromodulation 2024; 27: 476–488.

SUPPLEMENTARY DATA

To access the supplementary material accompanying this article, visit the online version of *Neuromodulation: Technology at the Neural Interface* at www.neuromodulationjournal.org and at https://doi.org/10.1016/j.neurom.2023.03.018.

REFERENCES

1. Habets JGV, Heijmans M, Kuijf ML, Janssen MLF, Temel Y, Kubben PL. An update on adaptive deep brain stimulation in Parkinson's disease. *Mov Disord*. 2018;33:1834–1843.
2. Little S, Pogosyan A, Neal S, et al. Controlling Parkinson's disease with adaptive deep brain stimulation. *J Vis Exp*. 2014;89:51403.
3. Ramirez-Zamora A, Giordano J, Gunduz A, et al. Proceedings of the Seventh Annual Deep Brain Stimulation Think Tank: Advances in Neurophysiology, Adaptive DBS, Virtual Reality, Neuroethics and Technology. *Front Hum Neurosci*. 2020;14:54.
4. Swann NC, de Hemptinne C, Aron AR, Ostrem JL, Knight RT, Starr PA. Elevated synchrony in Parkinson disease detected with electroencephalography. *Ann Neurol*. 2015;78:742–750.
5. Tinkhauser G, Pogosyan A, Little S, et al. The modulatory effect of adaptive deep brain stimulation on beta bursts in Parkinson's disease. *Brain*. 2017;140:1053–1067.
6. Arlotti M, Marceglia S, Foffani G, et al. Eight-hours adaptive deep brain stimulation in patients with Parkinson disease. *Neurology*. 2018;90:e971–e976.
7. Velisar A, Syrkin-Nikolau J, Blumenfeld Z, et al. Dual threshold neural closed loop deep brain stimulation in Parkinson disease patients. *Brain Stimul*. 2019;12:868–876.
8. Little S, Pogosyan A, Neal S, et al. Adaptive deep brain stimulation in advanced Parkinson disease. *Ann Neurol*. 2013;74:449–457.
9. Fleming JE, Dunn E, Lowery MM. Simulation of closed-loop deep brain stimulation control schemes for suppression of pathological beta oscillations in Parkinson's disease. *Front Neurosci*. 2020;14:166.
10. Santaniello S, Fiengo G, Glielmo L, Grill WM. Closed-loop control of deep brain stimulation: a simulation study. *IEEE Trans Neural Syst Rehabil Eng*. 2011;19:15–24.
11. Grado LL, Johnson MD, Netoff TI. Bayesian adaptive dual control of deep brain stimulation in a computational model of Parkinson's disease. *PLoS Comput Biol*. 2018;14:e1006606.
12. Rosin B, Slovik M, Mitelman R, et al. Closed-loop deep brain stimulation is superior in ameliorating parkinsonism. *Neuron*. 2011;72:370–384.
13. Johnson LA, Nebeck SD, Muralidharan A, Johnson MD, Baker KB, Vitek JL. Closed-loop deep brain stimulation effects on parkinsonian motor symptoms in a non-human primate - is beta enough? *Brain Stimul*. 2016;9:892–896.
14. Morin N, Jourdain VA, Di Paolo T. Modeling dyskinesia in animal models of Parkinson disease. *Exp Neurol*. 2014;256:105–116.
15. Dorval AD, Grill WM. Deep brain stimulation of the subthalamic nucleus reestablishes neuronal information transmission in the 6-OHDA rat model of parkinsonism. *J Neurophysiol*. 2014;111:1949–1959.
16. Badstuebner K, Gimsa U, Weber I, Tuchscherer A, Gimsa J. Deep brain stimulation of hemiparkinsonian rats with unipolar and bipolar electrodes for up to 6 weeks: behavioral testing of freely moving animals. *Parkinsons Dis*. 2017;2017:5693589.
17. Kocabicak E, Jahanshahi A, Schonfeld L, Hescham SA, Temel Y, Tan S. Deep brain stimulation of the rat subthalamic nucleus induced inhibition of median raphe serotonergic and dopaminergic neurotransmission. *Turk Neurosurg*. 2015;25:721–727.
18. Avila I, Parr-Brownlie LC, Brazhnik E, Castañeda E, Bergstrom DA, Walters JR. Beta frequency synchronization in basal ganglia output during rest and walk in a hemiparkinsonian rat. *Exp Neurol*. 2010;221:307–319.
19. Brazhnik E, Novikov N, McCoy AJ, Cruz AV, Walters JR. Functional correlates of exaggerated oscillatory activity in basal ganglia output in hemiparkinsonian rats. *Exp Neurol*. 2014;261:563–577.
20. Delaville C, McCoy AJ, Gerber CM, Cruz AV, Walters JR. Subthalamic nucleus activity in the awake hemiparkinsonian rat: relationships with motor and cognitive networks. *J Neurosci*. 2015;35:6918–6930.
21. Aulehner K, Bray J, Koska I, et al. The impact of tethered recording techniques on activity and sleep patterns in rats. *Sci Rep*. 2022;12:3179.
22. Lidster K, Jefferys JG, Blümcke I, et al. Opportunities for improving animal welfare in rodent models of epilepsy and seizures. *J Neurosci Methods*. 2016;260:2–25.
23. Lundt A, Wormuth C, Siwek ME, et al. EEG radiotelemetry in small laboratory rodents: A powerful state-of-the art approach in neuropsychiatric, neurodegenerative, and epilepsy research. *Neural Plast*. 2016;2016:8213878.
24. Brown AR, Antle MC, Hu B, Teskey GC. High frequency stimulation of the subthalamic nucleus acutely rescues motor deficits and neocortical movement representations following 6-hydroxydopamine administration in rats. *Exp Neurol*. 2011;231:82–90.
25. Huotarinen A, Penttinen AM, Bäck S, et al. Combination of CDNF and deep brain stimulation decreases neurological deficits in late-stage model Parkinson's disease. *Neuroscience*. 2018;374:250–263.
26. Polar CA, Gupta R, Lehmkuhle MJ, Dorval AD. Correlation between cortical beta power and gait speed is suppressed in a parkinsonian model, but restored by therapeutic deep brain stimulation. *Neurobiol Dis*. 2018;117:137–148.
27. Shi LH, Woodward DJ, Luo F, Anstrom K, Schallert T, Chang JY. High-frequency stimulation of the subthalamic nucleus reverses limb-use asymmetry in rats with unilateral 6-hydroxydopamine lesions. *Brain Res*. 2004;1013:98–106.
28. Yu C, Cassar IR, Sambangi J, Grill WM. Frequency-specific optogenetic deep brain stimulation of subthalamic nucleus improves parkinsonian motor behaviors. *J Neurosci*. 2020;40:4323–4334.
29. Capozzo A, Vitale F, Mattei C, Mazzone P, Scarnati E. Continuous stimulation of the pedunculopontine tegmental nucleus at 40 Hz affects preparative and executive control in a delayed sensorimotor task and reduces rotational movements induced by apomorphine in the 6-OHDA parkinsonian rat. *Behav Brain Res*. 2014;271:333–342.
30. Evers J, Sridhar K, Lowery M. Feasibility of pair-housing of rats after cranial implant surgery. *Lab Anim*. 2023;57:69–74.

31. Sotocinal SG, Sorge RE, Zaloum A, et al. The Rat Grimace Scale: a partially automated method for quantifying pain in the laboratory rat via facial expressions. *Mol Pain*. 2011;7:55.
32. Volkmann J, Moro E, Pahwa R. Basic algorithms for the programming of deep brain stimulation in Parkinson's disease. *Mov Disord*. 2006;21(suppl 14):S284–S289.
33. Koss AM, Alterman RL, Tagliati M, Shils JL. Calculating total electrical energy delivered by deep brain stimulation systems. *Ann Neurol*. 2005;58:168 [author reply: 168–169].
34. Bates D, Machler M, Bolker BM, et al. Fitting linear mixed-effects models using lme4. *J Stat Softw*. 2015;67:1–48.
35. Kuznetsova A, Brockhoff PB, Christensen RHB. lmerTest package: tests in linear mixed effects models. *J Stat Soft*. 2017;82:1–26.
36. Lenth RV, Bolker B, Buerkner P, Giné-Vázquez I, Herve M, Jung M, Love J, Miguez F, Riebl H, Singmann H. emmeans: estimated marginal means, aka least-squares means. Accessed February 25, 2022. project.org/web/packages/emmeans/index.html#:~:text=emmeans%3A%20Estimated%20Marginal%20Means%2C%20aka%20Least%2DSquares%20Means&text=Compute%20contrasts%20or%20linear%20functions,trends%2C%20and%20comparisons%20of%20slopes
37. Mallet N, Pogosyan A, Sharott A, et al. Disrupted dopamine transmission and the emergence of exaggerated beta oscillations in subthalamic nucleus and cerebral cortex. *J Neurosci*. 2008;28:4795–4806.
38. Boix J, von Hieber D, Connor B. Gait analysis for early detection of motor symptoms in the 6-OHDA rat model of Parkinson's disease. *Front Behav Neurosci*. 2018;12:39.
39. Carvalho MM, Campos FL, Coimbra B, et al. Behavioral characterization of the 6-hydroxidopamine model of Parkinson's disease and pharmacological rescuing of non-motor deficits. *Mol Neurodegener*. 2013;8:14.
40. Amoozegar S, Pooyan M, Roughani M. Toward a closed-loop deep brain stimulation in Parkinson's disease using local field potential in parkinsonian rat model. *Med Hypotheses*. 2019;132:109360.
41. Sharott A, Magill PJ, Harnack D, Kupsch A, Meissner W, Brown P. Dopamine depletion increases the power and coherence of beta-oscillations in the cerebral cortex and subthalamic nucleus of the awake rat. *Eur J Neurosci*. 2005;21:1413–1422.
42. Mottaghi S, Kohl S, Biemann D, et al. Bilateral intracranial beta activity during forced and spontaneous movements in a 6-OHDA hemi-PD rat model. *Front Neurosci*. 2021;15:700672.
43. Li M, Zhou M, Wen P, et al. The network of causal interactions for beta oscillations in the pedunculopontine nucleus, primary motor cortex, and subthalamic nucleus of walking parkinsonian rats. *Exp Neurol*. 2016;282:27–36.
44. Brown P. Abnormal oscillatory synchronisation in the motor system leads to impaired movement. *Curr Opin Neurobiol*. 2007;17:656–664.
45. Joundi RA, Brittain JS, Green AL, Aziz TZ, Brown P, Jenkinson N. Persistent suppression of subthalamic beta-band activity during rhythmic finger tapping in Parkinson's disease. *Clin Neurophysiol*. 2013;124:565–573.
46. Storzer L, Butz M, Hirschmann J, et al. Bicycling suppresses abnormal beta synchrony in the Parkinsonian basal ganglia. *Ann Neurol*. 2017;82:592–601.
47. Kühn AA, Kupsch A, Schneider GH, Brown P. Reduction in subthalamic 8–35 Hz oscillatory activity correlates with clinical improvement in Parkinson's disease. *Eur J Neurosci*. 2006;23:1956–1960.
48. Farokhniaee A, Marceglia S, Priori A, Lowery MM. Effects of contralateral deep brain stimulation and levodopa on subthalamic nucleus oscillatory activity and phase-amplitude coupling. *Neuromodulation*. 2023;26:310–319.
49. Brocker DT, Swan BD, So RQ, Turner DA, Gross RE, Grill WM. Optimized temporal pattern of brain stimulation designed by computational evolution. *Sci Transl Med*. 2017;9:eaah3532.
50. McNamara CG, Rothwell M, Sharott A. Stable, interactive modulation of neuronal oscillations produced through brain-machine equilibrium. *Cell Rep*. 2022;41:111616.
51. Li Z, Guo Y, Bao X, et al. Effects of subthalamic deep brain stimulation with different frequencies in a parkinsonian rat model. *Neuromodulation*. 2021;24:220–228.
52. Swan CB, Schulte DJ, Brocker DT, Grill WM. Beta frequency oscillations in the subthalamic nucleus are not sufficient for the development of symptoms of parkinsonian bradykinesia/akinesia in rats. *eNeuro*. 2019;6ENEURO.0089-19.2019.
53. Walsh RN, Cummins RA. The Open-Field Test: a critical review. *Psychol Bull*. 1976;83:482–504.
54. Bédard C, Kröger H, Destexhe A. Modeling extracellular field potentials and the frequency-filtering properties of extracellular space. *Biophys J*. 2004;86:1829–1842.
55. Buzsáki G, Anastassiou CA, Koch C. The origin of extracellular fields and currents–EEG, ECoG, LFP and spikes. *Nat Rev Neurosci*. 2012;13:407–420.
56. AlHinai N. Introduction to biomedical signal processing and artificial intelligence. In: *Biomedical Signal Processing and Artificial Intelligence in Healthcare*. Academic Press; 2020:1–28.
57. Little S, Beudel M, Zrinzo L, et al. Bilateral adaptive deep brain stimulation is effective in Parkinson's disease. *J Neurol Neurosurg Psychiatry*. 2016;87:717–721.
58. Rodriguez-Zurrunero R, Araujo A, Lowery MM. Methods for lowering the power consumption of OS-based adaptive deep brain stimulation controllers. *Sensors (Basel)*. 2021;21:2349.
59. Rosa M, Arlotti M, Ardolino G, et al. Adaptive deep brain stimulation in a freely moving Parkinsonian patient. *Mov Disord*. 2015;30:1003–1005.
60. Lu M, Wei X, Che Y, Wang J, Loparo KA. Application of reinforcement learning to deep brain stimulation in a computational model of Parkinson's disease. *IEEE Trans Neural Syst Rehabil Eng*. 2020;28:339–349.